

Magnetic interactions of Cr-Cr and Co-Co impurity pairs in ZnO within a band-gap corrected density functional approach

Stephan Lany, Hannes Raebiger, and Alex Zunger

National Renewable Energy Laboratory, Golden, Colorado 80401, USA

(Received 20 February 2008; revised manuscript received 29 April 2008; published 3 June 2008)

The well-known “band-gap” problem in approximate density functionals is manifested mainly in an overly low energy of the conduction band (CB). As a consequence, the localized gap states of $3d$ impurities states in wide-gap oxides such as ZnO occur often incorrectly as resonances inside the CB, leading to a spurious transfer of electrons from the impurity state into the CB of the host, and to a physically misleading description of the magnetic $3d$ - $3d$ interactions. A correct description requires that the magnetic coupling of the impurity pairs be self-consistently determined in the presence of a correctly positioned CB (with respect to the $3d$ states), which we achieve here through the addition of empirical nonlocal external potentials to the standard density functional Hamiltonian. After this correction, both Co and Cr form occupied localized states in the gap and empty resonances low inside the CB. In otherwise undoped ZnO, Co and Cr remain paramagnetic, but electron-doping instigates strong ferromagnetic coupling when the resonant states become partially occupied.

DOI: 10.1103/PhysRevB.77.241201

PACS number(s): 75.30.Hx, 75.50.Pp, 71.15.Mb

$3d$ impurities generally tend to render semiconductors insulating due to deep levels inside the gap,¹ in particular in wide-gap systems such as diluted magnetic oxides (DMO).² For the purpose of spintronics, however, it is desired to achieve spin-polarized electrons in a conductive state close to the conduction-band minimum (CBM).³ While ferromagnetic signatures are frequently observed in $3d$ doped ZnO and other wide-gap oxides, the origin and nature of the ferromagnetism (FM) remains enigmatic: For example, carrier (electron) mediated magnetism has been assumed in ZnO:Co on the basis of the correlation of magnetism with Al donor doping,⁴ or with the O₂ partial pressure controlling the conductivity.⁵ Other interpretations involve the formation of nanoclusters of the naturally magnetic Co metal,⁶ or uncompensated spins at the interface between paramagnetic Co-poor and antiferromagnetic (AFM) Co-rich phases of (Zn,Co)O, formed due to spinodal decomposition.⁷ Even more perplexing questions about the nature of ferromagnetism in DMO have been raised by recent reports showing that the $3d$ sublattice remains paramagnetic even though the sample as a whole appears ferromagnetic, as observed, e.g., in ZnO:Co (Ref. 8) and ZnO:Cu,⁹ and the observation that magnetism in polycrystalline thin-film ZnO occurs even without transition-metal doping.¹⁰

In the present study, we address theoretically the possibility of transition-metal (TM) induced ferromagnetism in *single-crystal* ZnO (note that this type of magnetism may be overshadowed in polycrystalline thin films or nanocrystals by a poorly understood magnetism that is independent of TM doping¹⁰). In light of the unclear experimental situation, numerous theoretical studies emerged on $3d$ impurities in oxides, using mostly the local-density or generalized-gradient approximations (LDA or GGA) to density functional theory (DFT).^{11–13} However, certain oxides such as ZnO or In₂O₃ have a large electron affinity (low CBM energy) that is further exaggerated in LDA/GGA calculations where the notorious band-gap underestimation (e.g., in ZnO, $E_g=0.73$ eV in GGA compared to 3.4 eV in experiment) is mainly due to a too low energy of the CBM.¹⁴ As shown below, these systematic errors cause the *highest occupied* level of most $3d$

impurities in ZnO to incorrectly appear as resonances inside the LDA/GGA host conduction band, leading to a spurious charge transfer from the $3d$ impurity level into the host bands, whereas a deep impurity level inside the gap is expected from experiment.^{3,15}

The need for a self-consistent band-gap correction. The magnetic $3d$ - $3d$ pair interaction energies in ZnO: $3d$ must be determined in the presence of corrected host band energies (relative to the impurity levels), so that the correct description of the orbital and spin configuration of the impurity is recovered during the self-consistent calculation. It is now recognized that Hubbard- U corrections¹⁶ to LDA or GGA significantly improve the description of the TM- d states in magnetic semiconductors,^{12,13,17} but as these corrections in general do not sufficiently open the band gap,¹⁸ they cannot remove the spurious hybridization of the $3d$ orbitals with the host conduction band. The need for both a self-consistent correction of the host band-edge energies and for an efficient computational scheme capable of calculating total-energy differences and atomic relaxations in fairly large supercells is the central challenge for the description of ferromagnetism in $3d$ doped wide-gap oxides. Due to these simultaneous requirements, accurate *ab initio* methods that avoid the band-gap problem, such as GW calculations,¹⁴ are currently not practical.

We achieve here a self-consistent band-gap correction by adding to the standard GGA+ U Hamiltonian empirical non-local external potentials (NLEP) $\Delta V_{\alpha,l}^{\text{NLEP}}$ that depend on the atomic type (α) and the angular momentum (l). This approach follows the spirit of the method of Christensen,¹⁹ but here we use angular-momentum-dependent (“nonlocal”) potentials²⁰ that allow for more flexibility in fitting experimental band-structure properties. The NLEP correction is implemented into the projector augmented wave (PAW) formalism²¹ within the VASP code²² (see below). The host-crystal NLEP parameters $\Delta V_{\text{Zn},s}=+9.4$ eV, $\Delta V_{\text{Zn},p}=-1.2$ eV, $\Delta V_{\text{O},s}=-6.4$ eV, and $\Delta V_{\text{O},p}=-2.0$ eV are obtained by fitting to target properties taken from experiment²³ and GW calculations,¹⁴ as summarized in Table I. (Note that negative values of ΔV imply an attractive potential, and posi-

TABLE I. Target properties used for the fit of the NLEP potentials. Band-structure parameters: The energy of the CBM, the conduction-band effective mass, the energy of the conduction band at the L point (from the GW calculation of Ref. 14), and the Zn- d band energies (all energies with respect to the VBM). Structural parameters: the unit cell volume, the c/a ratio, and the displacement parameter u .

	GGA	NLEP	target	
$E_C(\Gamma)$ (eV)	0.73	3.23	3.44	(expt.)
m^*/m_e	0.19	0.47	0.28	(expt.)
$E_C(L)$ (eV)	5.64	6.43	7.40	(GW)
Zn- d band (eV)	-4.8	-7.0	-8.8 to -7.5	(expt.)
Volume (\AA^3)	49.75	45.02	47.61	(expt.)
c/a	1.613	1.575	1.602	(expt.)
u	0.379	0.386	0.383	(expt.)

tive values imply a repulsive potential for the respective L component.) The main contribution to the band-gap correction comes from the repulsive Zn- s potential correction, in accord with the GW finding¹⁴ that most of the correction occurs through an upward shift of the conduction band, which has strong Zn- s character.²⁴ Other methods with similar capabilities of a self-consistent band-gap correction that have been applied to DMO are hybrid-DFT (Ref. 25) and approximate self-interaction correction (SIC) methods.^{26,27} We will compare our results to those methods below.

For the conventional GGA+ U Hamiltonian, we use the GGA parametrization of Ref. 28 and the rotationally invariant “+ U ” formulation of Ref. 16(b). The Hubbard- U parameters for the TM- d orbitals are determined according to Ref. 18 such that the thermochemically correct relative stability of the different oxide stoichiometries (e.g., CoO vs Co₃O₄) is obtained. Thus, we use $U=2.6, 3.9, 3.5, 2.8,$ and 3.4 eV for Cr, Mn, Fe, Co, and Ni, respectively, where the exchange parameter is set to the typical value of $J=1$ eV.¹⁶ As discussed in Ref. 18, these values are considerably smaller than the respective values that would reproduce the experimental band gaps of the TM oxides, which, however, should not be expected from the GGA+ U method. The larger value $U=7$ eV for Zn (d^{10}) (Ref. 29) compared to the TM reflects its deeper and more localized semicore d^{10} shell. The following results are obtained in supercells of 72 atoms, using an energy cutoff of 440 eV and a Γ -centered $4 \times 4 \times 4$ k mesh for Brillouin-zone integration. In the calculations with additional electron doping, we apply the general methodology for charged supercells, as described in Ref. 30.

We test the present (GGA+ U)+NLEP methodology by predicting defect properties that were not included in the fitting of the empirical parameters, namely the optical-absorption energies of several $3d$ impurities. By studying photoinduced changes in the electron paramagnetic resonance (EPR) spectrum, Jiang *et al.*¹⁵ concluded that light with $h\nu=1.96$ eV was able to excite electrons from the valence band of ZnO into the gap levels of the ionized (singly positively charged) transition metals for Mn(+III), Co(+III), and Ni(+III), but not for Fe(+III). Thus, we calculated, according to the description given in Ref. 29, the optical (ver-

TABLE II. The calculated $\varepsilon_O(+/0;h)$ excitation energy for the optical (vertical) transition $\text{TM}_{\text{Zn}}^+ \rightarrow \text{TM}_{\text{Zn}}^0 + h$, compared with the conclusions-obtained from photo-EPR experiments (Ref. 15) using 633 nm light ($h\nu=1.96$ eV). The respective thermodynamic (relaxed) $\varepsilon(+/0)$ transition levels are also given. All numbers in eV.

		Mn	Fe	Co	Ni
NLEP	$\varepsilon_O(+/0;h)=$	1.20	2.83	0.96	1.69
Expt. (Ref. 15)	$\varepsilon_O(+/0;h)$	≤ 1.96	> 1.96	≤ 1.96	≤ 1.96
NLEP	$\varepsilon(+/0)-E_{\text{VBM}}=$	0.48	1.96	0.31	0.67

tical) transition energy $\varepsilon_O(+/0;h)$, which is defined as the threshold photon energy required for the excitation $\text{TM}_{\text{Zn}}^+ \rightarrow \text{TM}_{\text{Zn}}^0 + h$ (oxidation states: $\text{TM}_{\text{Zn}}^{+\text{III}} \rightarrow \text{TM}_{\text{Zn}}^{+\text{II}} + h$). As seen in Table II, the NLEP approach reproduces the experimental observations. For completeness, we also give in Table II the calculated thermodynamic (thermal) transition levels $\varepsilon(+/0)$ (see, e.g., Ref. 30). Finally, we note that our $\varepsilon(+/0)=E_{\text{VBM}}+0.31$ eV transition energy for Co_{Zn} lies considerably lower in the gap than the respective 2.9 eV level found in Ref. 26, where the band-gap correction was achieved by treating the Zn- d shell as frozen-core electrons, and where self-interaction corrections were applied only to

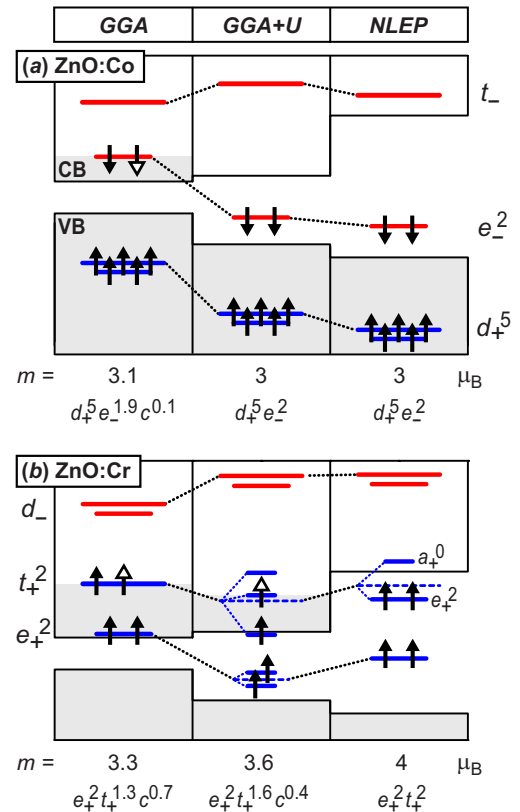


FIG. 1. (Color online) Orbital and spin configuration of (a) Co_{Zn} and (b) Cr_{Zn} in ZnO and the resulting magnetic moment m in GGA, in GGA+ U (for Zn- d , Co- d , and Cr- d), and in the fully gap-corrected NLEP method. Charge transfer from occupied TM- d states into the host conduction band (e.g., $e^- \rightarrow e_{-}^{1.9} c^{0.1}$ for Co_{Zn} in GGA) is indicated by open arrow symbols. Dashed lines in (b) indicate the average level energy before the Jahn-Teller splitting.

the Co-*d* shell. A $\epsilon(+/0)$ level higher than $E_{\text{VBM}}+1.96$ eV is, however, inconsistent with the conclusion obtained from the photo-EPR experiments.¹⁵

Orbital and spin configuration of single Co and Cr impurities. Figure 1 shows the calculated orbital and spin configuration of single, charge-neutral Co_{Zn} and Cr_{Zn} impurities in ZnO at the levels of uncorrected GGA, of GGA+*U* and of fully gap-corrected NLEP.

For Co_{Zn} in the GGA description [Fig. 1(a)], the doubly occupied e_- minority-spin level occurs as a resonance inside the (uncorrected) GGA conduction band, leading to a charge transfer of $0.1e$ into the ZnO host conduction band for the 72-atom supercell. Accordingly, Co_{Zn} effectively forms an $e_-^{1.9}c^{0.1}$ configuration with a noninteger total magnetic moment $m=3.1\mu_B/\text{Co}$ at this Co concentration (10^{21} cm^{-3}). Using the GGA+*U* description for the Zn-*d* orbitals of the ZnO host, the band gap is increased mostly by lowering the energy of the valence-band maximum.²⁹ The simultaneous application of *U* to the Co-*d* states increases the splitting between occupied e_- and the unoccupied t_- minority-spin levels (the symmetry labels *e* and *t* refer to the approximate local tetrahedral symmetry). Thus, in GGA+*U*, the e_- level occurs correctly inside the gap, leading to an integer moment, but the unoccupied t_- level creates a resonance that is still far too high above the CBM [Fig. 1(a)]. After additional application of the NLEP correction, which recovers the correct magnitude of the band gap mostly by raising the energy of the conduction bands, the unoccupied resonance of the t_- level of Co_{Zn} lies close to the CBM at about $E_C+0.5$ eV [Fig. 1(a)]. Comparing our NLEP result to recent band-gap corrected hybrid-DFT (Ref. 25) and SIC (Ref. 27) calculations, we find that the t_- resonance occurs slightly higher at E_C+1 eV in SIC,²⁷ and considerably higher above E_C+2 eV in hybrid-DFT.²⁵ The proximity of the t_- level to the CBM will turn out to be important when considering the addition of electrons via *n*-type doping (see below).

For Cr_{Zn} impurities [Fig. 1(b)] in the GGA description, the resonance of the *occupied* majority-spin t_+^2 level lies deep inside the conduction band in GGA, at about $E_C+1.2$ eV, leading to a large charge transfer of $0.7e$ into the host conduction band and to an electron configuration $e_+^{2.3}t_+^{1.3}c^{0.7}$. Accordingly, we find a noninteger total magnetic moment $m=3.3\mu_B$ per supercell, much smaller than the expected $4\mu_B$ [Fig. 1(b)]. As expected from the partial occupancy of the t_+ level, there exists a Jahn-Teller effect, manifested by splitting of the e_+ and t_+ levels by ~ 0.2 eV [not shown in Fig. 1(b)]. In the GGA+*U* description, the Jahn-Teller effect is strongly enhanced, and we observe the splitting of the t_+ level into three sublevels, spread by 1.4 eV. The lower-energy e_+ level is now split by 0.3 eV due to breaking of the C_{3v} symmetry. Since one occupied sublevel lies still inside the GGA+*U* conduction band, there is again a charge transfer to the host conduction band leading to a noninteger moment of $m=3.6\mu_B$ and an effective $e_+^{2.1.6}t_+^{1.6}c^{0.4}$ configuration. The spurious charge transfer into the host band is avoided only after full correction of the band gap in NLEP, where the correct $e_+^2t_+^2$ configuration and the integer moment of $4\mu_B$ of Cr(+II) are recovered. Since the nominal t_+^2 configuration is realized in this case, the Jahn-Teller effect leads to a different atomic structure than in GGA+*U*, such that the splitting

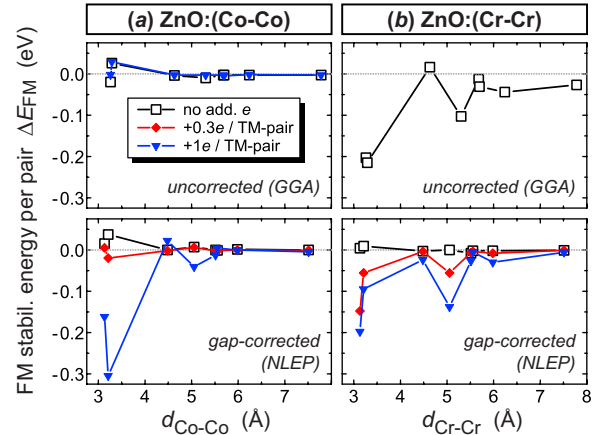


FIG. 2. (Color online) The ferromagnetic stabilization energy $\Delta E_{\text{FM}}=E_{\text{FM}}-E_{\text{AFM}}$ in eV for (a) the Co-Co and (b) the Cr-Cr pairs in a 72-atom ZnO supercell, as a function of the pair distance d . Results are given for the uncorrected GGA and for the gap-corrected NLEP methods, and for different levels of additional electron doping up to $1e$ per TM pair ($\sim 10^{21}\text{ cm}^{-3}$).

$t_+^2 \rightarrow e_+^2 + a_+^0$ [cf. Fig. 1(b)] does not lift the degeneracy of the *e* symmetries (the C_{3v} symmetry of wurtzite is preserved). Thus, in contrast to the case of Co_{Zn} , where the correct orbital and spin configuration is obtained already at the GGA+*U* level, for Cr_{Zn} the correct electron configuration and atomic structure of Cr_{Zn} are obtained only after the full band-gap correction in NLEP.

Magnetic Co-Co and Cr-Cr pair interactions. We now compare the FM stabilization energies $\Delta E_{\text{FM}}=E_{\text{FM}}-E_{\text{AFM}}$ for Co-Co and Cr-Cr pairs in 72-atom supercells considering uncorrected GGA and fully band-gap corrected NLEP.

For Co-Co pairs [Fig. 2(a)], both GGA and NLEP predict rather small differences $|\Delta E_{\text{FM}}| < 0.05$ eV between the FM and AFM states, similar to the case of the uncorrected LDA (Ref. 11) and the gap-corrected LDA+SIC calculations of Ref. 27. We next study the pair interactions in the presence of additional electrons that can be supplied in ZnO through *n*-type doping.⁴ Whereas in the uncorrected GGA calculation the addition of $1e$ per Co-Co pair (10^{21} cm^{-3} doping level) does not significantly affect the FM coupling energies, in the NLEP calculation electron doping induces a strong FM interaction between close pairs [Fig. 2(a)], showing that the band-gap correction is essential to obtain ferromagnetism in electron-doped ZnO:Co. This FM coupling occurs when the resonant t_- level of Co_{Zn} becomes partially occupied at high doping levels, conforming with the general expectation¹⁷ that partial occupancy of spin-polarized orbitals promotes ferromagnetism. In the recent SIC calculation of Ref. 27, where the t_- resonance occurs at somewhat higher energy (see above), FM coupling of Co-Co would require higher electron concentrations than in the present work. It was found in Ref. 27, however, that pairing of Co_{Zn} with O vacancies lowers the t_- level, allowing for long-range ferromagnetism at achievable electron densities. In contrast, in an uncorrected GGA or in a GGA+*U* calculation, no partial occupation of the t_- level is achieved at realistic doping levels,¹¹ because due to the too low CBM energy [Fig. 1(a)], the additional electrons populate the host conduction band instead of the t_- defect level of Co_{Zn} .

For Cr-Cr pairs [Fig. 2(b)], the uncorrected GGA calculation erroneously predicts a strong and long-range FM coupling between Cr pairs even when no additional electrons are supplied [Fig. 2(b)]. This prediction of magnetism originates from the spurious partial occupancy of the t_+ level of Cr being resonant inside the uncorrected GGA conduction band [see Fig. 1(b)]. In contrast, in the band-gap corrected NLEP calculation, this partial occupancy is removed by the Jahn-Teller effect [Fig. 1(b)], and the ensuing FM coupling energies ΔE_{FM} become small [Fig. 2(b)]. When electrons are added through doping, the unoccupied Jahn-Teller split a_+ state in the conduction band becomes partially occupied, leading to strong and long-ranged FM coupling that increases with the amount of doping [Fig. 2(b)]. Thus, also in ZnO:Cr, the supply of additional electrons is essential for FM coupling.

Technical description of the NLEP implementation. In the PAW method,^{21,22} the all-electron (AE) wave functions ψ^{AE} are reconstructed from the pseudo- (PS) wave functions ψ^{PS} by means of a linear transformation,

$$|\psi^{\text{AE}}\rangle = |\psi^{\text{PS}}\rangle + \sum_i (|\phi_i^{\text{AE}}\rangle - |\phi_i^{\text{PS}}\rangle) \langle p_i | \psi^{\text{PS}} \rangle,$$

using a set of projector functions p_i . Here, the index i comprises the individual atomic sites, the angular-momentum quantum numbers l, m and the reference energies (usually two per l), which are used in the atomic reference calculation to construct the partial waves ϕ_i^{AE} and ϕ_i^{PS} , and the pseudo-potential. Similarly, the AE potential operator is obtained in the PAW method as^{21,22}

$$V^{\text{AE}} = V^{\text{PS}} + \sum_{i,j} |p_i\rangle \langle (\phi_i^{\text{AE}} | V^{\text{AE},1} | \phi_j^{\text{AE}}) - \langle \phi_i^{\text{PS}} | V^{\text{PS},1} | \phi_j^{\text{PS}} \rangle \langle p_j|,$$

where $V^{\text{AE}}, V^{\text{PS}}$ are the “global” effective Kohn-Sham potentials (ionic+Hartree+exchange correlation), and $V^{\text{AE},1}, V^{\text{PS},1}$ are their respective one-center expansions within the augmentation spheres. The NLEP potentials $\Delta V_{\alpha,l}^{\text{NLEP}}$ for the atomic types α and the angular momenta l are added to the AE one-center potential,

$$V^{\text{AE},1} \rightarrow V^{\text{AE},1} + \Delta V_{\alpha,l}^{\text{NLEP}} \delta_{l,l(i)} \delta_{l(i),l(j)},$$

where $l(i)$ and $l(j)$ are the l subindices within i and j .

Conclusions. Due to the band-gap problem exhibited by the LDA and GGA functionals, and their “+ U ” extensions, these methods may predict the absence of FM coupling where such coupling is expected to exist (e.g., ZnO:Co +electron doping), or may predict FM coupling where such coupling should not exist (e.g., ZnO:Cr). For the correct description of magnetism in wide-gap oxides such as ZnO, it is essential to recover the correct band-edge energies of the host in a self-consistent manner. Determining ferromagnetic coupling energies for Co-Co and Cr-Cr pairs in ZnO within a fully band-gap corrected method using empirical nonlocal external potentials, we find that both Co and Cr show paramagnetic behavior in the absence of additional carriers, but ferromagnetic coupling occurs when sufficient additional electrons are supplied such that the initially unoccupied resonant defect levels of Co and Cr inside the conduction band become partially occupied.

This work was funded by the DARPA PROM program and the U.S. Department of Energy, Office of Energy Efficiency and Renewable Energy, under Contract No. DE-AC36-99GO10337 to NREL.

- ¹V. F. Masterov, Fiz. Tekh. Poluprovodn. (S.-Peterburg) **18**, 3 (1984) [Sov. Phys. Semicond. **18**, 1 (1984)].
- ²J. Osorio-Guillén, S. Lany, and A. Zunger, Phys. Rev. Lett. **100**, 036601 (2008).
- ³K. R. Kittilstved, W. K. Liu, and D. R. Gamelin, Nat. Mater. **5**, 291 (2006).
- ⁴A. J. Behan *et al.*, Phys. Rev. Lett. **100**, 047206 (2008).
- ⁵K. R. Kittilstved *et al.*, Phys. Rev. Lett. **97**, 037203 (2006).
- ⁶K. Rode *et al.*, Appl. Phys. Lett. **92**, 012509 (2008).
- ⁷T. Dietl *et al.*, Phys. Rev. B **76**, 155312 (2007).
- ⁸A. Barla *et al.*, Phys. Rev. B **76**, 125201 (2007).
- ⁹D. J. Keavney *et al.*, Appl. Phys. Lett. **91**, 012501 (2007).
- ¹⁰N. H. Hong, J. Sakai, and V. Brizé, J. Phys.: Condens. Matter **19**, 036219 (2007).
- ¹¹E. C. Lee *et al.*, Phys. Rev. B **69**, 085205 (2004); K. Sato *et al.*, Phys. Status Solidi B **229**, 673 (2002). Using the GGA and LDA functionals for ZnO:Co, these authors found significant FM coupling only at very high concentrations of Co impurities and additional electrons (up to 25% or 10^{22} cm⁻³) compared to the present work (up to 3% or 10^{21} cm⁻³). At such unrealistically high Fermi levels, the t_- level of Co_{Zn} may be partially occupied despite its high energy at E_C+2 eV in GGA [see Fig. 1(a)].
- ¹²P. Gopal and N. A. Spaldin, Phys. Rev. B **74**, 094418 (2006).
- ¹³T. Chanier *et al.*, Phys. Rev. B **73**, 134418 (2006).
- ¹⁴M. Usuda *et al.*, Phys. Rev. B **66**, 125101 (2002).

- ¹⁵Y. Jiang, N. C. Giles, and L. E. Halliburton, J. Appl. Phys. **101**, 093706 (2007).
- ¹⁶V. I. Anisimov *et al.*, Phys. Rev. B **48**, 16 929 (1993); A. I. Liechtenstein *et al.*, *ibid.* **52**, R5467 (1995).
- ¹⁷P. Mahadevan *et al.*, Phys. Rev. Lett. **93**, 177201 (2004); P. Mahadevan *et al.*, Phys. Rev. B **69**, 115211 (2004).
- ¹⁸S. Lany, J. Osorio-Guillén, and A. Zunger, Phys. Rev. B **75**, 241203(R) (2007).
- ¹⁹N. E. Christensen, Phys. Rev. B **30**, 5753 (1984).
- ²⁰L. W. Wang, Appl. Phys. Lett. **78**, 1565 (1991).
- ²¹P. E. Blöchl, Phys. Rev. B **50**, 17 953 (1994).
- ²²G. Kresse and D. Joubert, Phys. Rev. B **59**, 1758 (1999).
- ²³*Semiconductors: Data Handbook*, 3rd ed., edited by O. Madelung (Springer, Berlin, 2004).
- ²⁴See EPAPS Document No. E-PRBMDO-77-R12820 for additional discussion of the band-gap correction with NLEP. For more information on EPAPS, see <http://www.aip.org/pubservs/epaps.html>
- ²⁵C. H. Patterson, Phys. Rev. B **74**, 144432 (2006).
- ²⁶L. Petit *et al.*, Phys. Rev. B **73**, 045107 (2006).
- ²⁷C. D. Pemmaraju *et al.*, arXiv:0801.4945v1.
- ²⁸J. P. Perdew, K. Burke, and M. Ernzerhof, Phys. Rev. Lett. **77**, 3865 (1996).
- ²⁹S. Lany and A. Zunger, Phys. Rev. B **72**, 035215 (2005).
- ³⁰C. Persson *et al.*, Phys. Rev. B **72**, 035211 (2005).